1

Non-Coronary Vessel Exploration Under Intravascular Ultrasound: Principles and Applicability

Gaël Y. Rochefort
Inserm U658 Ipros Chro, Orleans
France

1. Introduction

Intravascular Ultrasound (IVUS) has become rapidly one of the gold technologies for the endovascular exploration. Next to angiography, which only gives information about the lumen of the investigated vessels, IVUS describes both the luminal and trans-mural anatomy of vascular structures. Actual devices offer several configurations and transducers mounted at the end of an intra-luminal catheter to produce real-time grayscale or color images of blood vessels and cardiac structures. The ultrasound probes miniaturization has permitted closer imaging and magnified details of the vessel wall and plaque. Recent IVUS catheters use phased array imaging where the micro-transducers are enveloped around a catheter tip. Typically, IVUS images show the vessel wall in histological detail: the intima reflects ultrasound brightly and is white, the media is echolucent and dark, and the surrounding adventitia is white.
IVUS has thus become a safe and valuable tool in exploring the disease severity and the treatment completeness during surgical endovascular procedures (Jinzaki et al., 1993; Nishanian et al., 1999), such as assessing the severity of an arterial disease before treatment (Scoccianti et al., 1994), determining the plaque morphology and localization or checking the completeness of stent deployment (Diethrich, 1993; Laskey et al., 1993). Very recently, color flow IVUS and three-dimensional (3D) reconstruction have both introduced significant advances in the understanding of IVUS images (Irshad et al., 2001; Reid et al., 1995; White et al., 1994). The very latest advance, called virtual histology IVUS, provides a color-coded map of the plaque components, thus providing a better understanding of the arterial plaque structure and morphology (Nair et al., 2001; Vince & Davies, 2004).

2. IVUS principle

IVUS gives series of tomographic images of the explored vessel wall. During acquisition, an IVUS catheter is entered into a vessel and then withdrawn through a given vessel segment during simultaneous and continuous imaging, resulting in series of cross section images. Current catheters have frequencies from 30 to 40 MHz, planar resolutions from 50 to 150 μm, and a typical sampling rate of 30 images per second (Di Mario et al., 1995).

2.1 Acquisition using pullback devices

The current methods used to quantify a volumetric IVUS analysis are usually achieved by a simple summation of a targeted subsample of the 2-D images into a volumetric dataset (Chandrasekaran et al., 1994; Rosenfield et al., 1992; Rosenfield et al., 1991). In that case, the accurate volume calculations need the precise localization of each 2-D cross-sectional image used in the longitudinal axis of the vessel segment (Di Mario et al., 1995; Roelandt et al., 1994). To do so, a manual pullback was firstly performed, with recording of the time and length of the acquisition, and the image location was estimated from the pullback start point and the average pullback velocity. Alternatively, displacement sensors were used to record the IVUS catheter translation during the manual pullback procedure (Hagenaars et al., 2000). Since it is obviously difficult to maintain a consistent speed during manual pullback, most current systems have introduced a motorized pullback device with a constant speed (usually around 0.5 mm/s) (Cavaye et al., 1992; Liu et al., 1999; Matar et al., 1994).

2.2 Cardiac synchronization and frame selection

Since images are recorded at 30 frames per second, with a pullback speed of 0.5 mm/s, 60 frames are recorded for each 1-mm vessel segment. Since, a coronary segment of 3 to 10 cm is typically explored, 1800 to 6000 individual frames are usually recorded. Therefore, these large datasets are often sub-sampled using constant intervals (0.5 - 1.0 mm) or using an electrocardiogram gating: the 1-mm interval without respect to the cardiac cycle is often used for manual analysis, whereas computerized algorithms require different sampling intervals (Klingensmith et al., 2000a; von Birgelen et al., 1996a). Therefore, consecutive frames sub-sampled with a 1-mm interval are corresponding to changes in the lumen and vessel areas during the different phases of the cardiac cycle.

A typical “sawtooth” artifact can be seen on longitudinal 2-D pullback displays when the sub-sampling is performed without synchronization to the cardiac cycle. This sawtooth artifact is less marked when the explored vessel exhibit a reduced compliance (such as stented vessels or stenotic vessels). Nevertheless, it is recommended to get the cardiac cycle synchronization since it allows the cyclic cycle artifacts to be eliminated (von Birgelen et al., 1996b; von Birgelen et al., 1997b). In fact, different physiologic, cyclic signals are commonly used to synchronize the IVUS images to the cardiac cycle, including the arterial blood pressure and the electrocardiogram signals (Allan et al., 1998; Sonka et al., 1998).

When operating a retrospective gating, IVUS images and electrocardiogram signals are acquired continuously, since the electrocardiogram signals are required to sort the images and to perform the analysis of the volumetric dataset (Klingensmith et al., 2000a; Kovalski et al., 2000). On the other hand, when operating a prospective gating, the IVUS images are only acquired at a given times of the cardiac cycle and the catheter is then moved to acquire the next gated image (Bruining et al., 1998; von Birgelen et al., 1997a; von Birgelen et al., 1995). This last gating method presents the advantage to not requiring additional steps to perform the analysis of the dataset, and a volumetric dataset is available immediately after the acquisition pullback.

2.3 Transferring the IVUS dataset to an analysis system

The whole raw IVUS data, composed of the reflected acoustic signals, are displayed on IVUS consoles. This dataset could also be stored on S-VHS videotape, on CD-ROM or magneto-optical disks. Recent IVUS consoles have digital output capabilities that allow direct data

transfer in digital format, and may provide radiofrequency outputs composed of raw IVUS acoustic signals. This signal processing approach is particularly adapted for a computerized image analysis, since it allows traditional measurements but also radiofrequency-based tissue characterization (Nair et al., 2001; Nair et al., 2002).

3. Devices, recording methods and techniques

3.1 Devices

Typical mechanical IVUS transducers produce cross-sectional images by rotating at the tip of the catheter using a flexible, high-torque cable. These transducers are creating a cone-shaped ultrasound beam that allows the vessel to be imaged slightly forward or in front of the transducer assembly.

An optimized visualization is obtained when using IVUS catheter having appropriate size and frequency. Thus, the clinician has to make a compromise between the highest frequency *vs.* depth of penetration *vs.* catheter size. He also has to consider the wire guide diameter and the guide-wire exchanges utility. IVUS catheters used for most aortic and iliac procedures can be advanced over a 0.035-inch guide wire and range in size and frequency from 6 to 8 Fr and 8 to 20 MHz, respectively. An IVUS probe, ranging between 8 to 15 MHz is commonly used for aortic procedures, allowing an adequate circumferential imaging. The following Table 1 is presenting the current available catheters applicable for peripheral vascular and coronary interventions.

Intravascular Ultrasound Catheters	Size (Fr)	Guide Wire (in)	Frequency (MHz)	Target vessel
Volcano Corporation catheters (phase array)				
Eagle Eye Gold IVUS Imaging (color-flow and virtual histology)	3.5	0.014	20	Carotid renal iliac Femoral
Visions PV 0.018 F/X IVUS Imaging (color-flow)	3.5	0.018	20	Femoral popliteal tibial
Visions PV 8.2F IVUS Imaging	8.2	0.038	8.3	Aorta iliac
Boston Scientific catheters (rotating crystal)				
Atlantis SR Pro	3.2	0.014	40	Femoral popliteal tibial
Atlantis SR Plus	3	0.014	40	Femoral popliteal tibial
Atlantis SR	3.2	0.014	40	Femoral popliteal tibial
Atlantis PV Peripheral Imaging	8	0.035	15	Aorta iliac
Sonicath Ultra Ultrasound	9	0.035	9	Aorta iliac
Sonicath Ultra Ultrasound	3.2	0.018	20	Femoral popliteal tibial
Sonicath Ultra Ultrasound	6	0.035	12.5	Iliac femoral
Sonicath Ultra Ultrasound	6	0.035	20	Femoral popliteal tibial

Table 1. Specifications of commonly used intravascular ultrasound (IVUS) catheters in peripheral occlusive interventions.

3.2 Access to vessels

Depending on the size of the considered vessel (see Table 1), IVUS catheters can be introduced percutaneously through a standard vascular access sheath (5 to 9 Fr). The 8.2 Fr, 10-MHz catheter is one of the most commonly used catheter for aorta-iliac intervention, since it requires a 0.035-inch guide wire and thus can be quickly prepared, introduced, and/or exchanged with other catheters. However, this specific catheter requires a 9 Fr sheath that can be disproportionate for lower extremity interventions.

Most current percutaneous trans-luminal angioplasty balloons and stents targeted for infra-inguinal regions require only 6 Fr sheaths. The 3.4 Fr, 3.2 Fr, or 2.9 Fr catheters, using 0.018-inch and 0.014-inch guide wires, are more suitable for the typical retrograde common femoral artery puncture and access to the contra-lateral femoral-popliteal segments (Hiro et al., 1998; Saketkhoo et al., 2004). In some case, especially with tortuous vessels and when antegrade puncture of the common femoral vessel is required, the 3 Fr catheters are also useful.

Lengths of IVUS catheters are vary from 90 to 150 cm, thus allowing imaging of small tibial vessels from a contra-lateral up-and-over approach. The smaller catheters require 0.018-inch or 0.014-inch guide wires and are commonly used for infra-inguinal interventions, whereas the larger IVUS catheters need 0.035-inch guide wires and used for larger vessel interventions (Hiro et al., 1998).

3.3 Image acquisition and quality

An optimal visualization requires a careful positioning of the catheter tip within the vessel and an appropriate size matching of the device to the artery caliber, meaning that an IVUS intervention necessitates a pre-procedural estimation the target vessel diameters (Figure 1). The best image quality is obtained when the IVUS catheter is parallel to the vessel wall and when the ultrasound beam is perpendicular to the luminal surface. Some artificial differences in the wall thickness measurement may be obtained when the IVUS catheter has an eccentric position, leading to the vessel wall to appear more hyperechoic than the distant wall. Angulations may promote an elliptical image of the vessel lumen, especially when

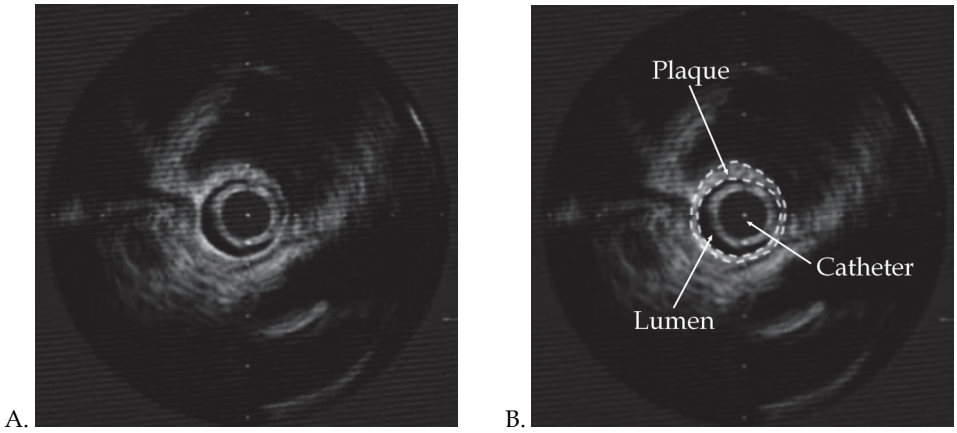

Fig. 1. Illustration of quantitative measurements with IVUS. Examples show an *in vivo* IVUS image digitized from video (A) and the detected borders overlaid (B).

considering tortuous aortas and the thoracic arch. In such cases, the minimal diameter (minor axis) is the best accurate measurement to measure the vessel diameter in angled images and/or tortuous vessels (Roelandt et al., 1994). At last, withdrawing the catheter through the lumen, rather than advancing it, promotes the acquisition of the best-quality images (Danilouchkine et al., 2009).
During the procedure, real-time images of the investigated vessel are displayed on a monitor and are usually recorded digitally. The IVUS devices also allow the on-line and/or off-line measurements of vessel dimensions, luminal diameters, and cross-sectional areas. Recent IVUS units, comprising a motorized and/or automated withdrawing the catheter through the vessel at a controlled rate, may display a longitudinal gray-scale image of the investigated vessel with accurate reconstructed views (Hagenaars et al., 2000). These two-dimensional longitudinal reconstructions allow distances to be measured from one point to another (Liu et al., 1999) and cross-sectional trans-mural wall morphology to be visualized (Di Mario et al., 1995). In fact, the discrimination of plaque, normal tissue, thrombus, dissections, and flaps is often much better appreciated on the two-dimensional longitudinal IVUS reconstructions than on traditional angiographic images (Reid et al., 1995).

4. Data processing and analysis

The dataset for volumetric analysis is represented by image series composed of two-dimensional sections from the investigated vessels. Typically, images are selected at 1-mm inter-slice spacing. Then, to perform a quantitative 3-D reconstruction, the first and most critical step is to precisely identify and trace the anatomical structures of the studied vessel. In fact, identifying the luminal border is essential to discriminate the blood-intima interface, whereas recognizing the external elastic membrane border is important to precisely distinguish the boundary between the media and the adventitia (Kovalski et al., 2000). The space between these 2 borders is the plaque-media complex and is classically used as the measurement for plaque cross-sectional area (Prati et al., 2002).
In stented vessel segments, the lumen/intimal interface and the stent borders are both measured, and the area between these borders is representing the neointimal tissue. In these stented vessel segments, the external elastic membrane border is frequently not distinguished because of signal drop-out behind the stent. In current atherosclerosis research trials, the assessment of stent, luminal and external elastic membrane borders is often performed with manual planimetry using commercially or freely available computer programs. This provides the accurate discrimination of image artifacts and true border locations but this analysis requires the border detection in hundreds of images. Therefore, the use of automated image-processing techniques allows fast online analysis (Sanz-Requena et al., 2007).

4.1 Automated 2-D/3-D border-detection methods

Different approaches have been described to detect the luminal and external elastic membrane borders from 2-D IVUS images, including texture-based methods (Papadogiorgaki et al., 2007), knowledge-based graph searching (Bovenkamp et al., 2009), region growing (Sanz-Requena et al., 2007), radial gradient searching (Luo et al., 2003), and active contours (Sanz-Requena et al., 2007; Takagi et al., 2000). These 2-D border-detection techniques are now used online in newer IVUS imaging consoles, allowing the quantitative evaluation of lumen and plaque measurements. Because the user provides his expertise to augment the algorithm or correct results, the semi-automated techniques typically require

more time but are have a better accuracy. These 2-D border-detection methods are particularly used when the analysis of only a small number of images is required, e.g. during the guidance of interventional procedures (Sarno et al., 2011).
When a fast analysis of many images is required, highly automated techniques for border detection are used and do not require significant user intervention. For example, 3-D border-detection methods using the inter-slice information can provide fast border detection from a large number of images (Cardinal et al., 2010). A graph-searching approach researching the globally optimal contour path through the image data has been developed on the basis of associated cost values (Zhang et al., 1998). Furthermore, this 2-D frame analysis method allows the results to be propagated down the sequence by using the identified 2-D contours in order to limit the search region. Another 2-D border-detection method uses cost values to find longitudinal contours along the volumetric data. Then, these contours guide the cost function minimization in the transverse 2-D images (Koning et al., 2002). Alternatively, several useful approaches use deformable models to perform an active contour detection (Klingensmith et al., 2000a; Kovalski et al., 2000) (Shekhar et al., 1999). One of them uses a balloon force to inflate a model from the catheter outward toward the luminal and medial-adventitial borders (Kovalski et al., 2000). Another deformable model uses a cylindrical model to manually or automatically approximate the structure of the luminal or medial-adventitial surface, and a deformable model algorithm is then used in a 3-D process to attach the defined structure to the surface of interest (Klingensmith et al., 2000a; Shekhar et al., 1999). All these methods allowing the 3-D border-detection have clearly established their overall usefulness for fast border identification in a large sequence of images (Klingensmith et al., 2000a; Kovalski et al., 2000; Shekhar et al., 1999; von Birgelen et al., 1996a; Zhang et al., 1998).
A major limitation of all these 3-D border-detection methods is the lack of a true gold standard for comparison. Histology sections might represent the more powerful gold standard, but they are only available at autopsy, and the required fixation always induces the tissue to shrink (Siegel et al., 1985). Some researchers have tried to evaluate the accuracy of their methods using cylindrical phantoms, but they did not test accuracy in clinical IVUS images (von Birgelen et al., 1996a). Other studies have compared the detected borders with borders traced manually by a single expert, but the obtained inter-observer variability in manual identification of the luminal and medial-adventitial borders might greatly limit the value of these comparisons in IVUS images (Haas et al., 2000; Zhang et al., 1998). At last, some studies have used multiple expert observers for validation, but the number of analyzed images is seriously limited and not sufficient to assess the ability and accuracy of these algorithms (Klingensmith et al., 2000a; Kovalski et al., 2000; Shekhar et al., 1999). Therefore, there is a need of validation of these techniques in large datasets.

4.2 3-D reconstructions of vessel segments

All measurements and evaluations made in 2-D tomographic slices are useful for stent sizing or comparisons of lesions to a reference site, but fail to provide a volumetric perspective. To do such volumetric calculations, the border measurements obtained in consecutive 2-D slices of a vessel segment are integrated, the area enclosed by the luminal border and external elastic membrane border is considered for each slice, and the atheroma area is calculated. The 3-D measurement of lumen, plaque, and vessel volumes are usually calculated with Simpson's rule or trapezoidal integration by the multiplying 2-D area and slice thickness (Finet et al., 2003; von Birgelen et al., 1997a). This last method is suitable for

short and straight vessel segments, such as coronary stented lesions, but it does not allow the precise measurement of a longer and curved segment.
The volumetric approach using 3-D border-detection techniques is currently applied in serial IVUS studies examining atherosclerotic disease progression or regression, allowing the assessment of plaque burden in an entire vessel segment through fast analysis of large image sequences. New interventional approaches also use a volumetric IVUS imaging approach to provide new mechanistic insights, such as innovative techniques aimed at the prevention and treatment of in-stent restenosis correlated with histomorphometry measurements (Mehran et al., 1998; Murata et al., 2002); approaches in understanding the effects of radiation therapy and the arterial remodeling on a stented segment (brachytherapy) (Lekston et al., 2008; Weichert et al., 2003; Zimarino et al., 2002; Zimmermann et al., 2005); or using drug-eluting stents on the neointimal hyperplasia development (Jensen et al., 2008; Min et al., 2007; Sano et al., 2006).

4.3 Geometrically correct 3-D IVUS and advanced data processing

Since the curvature of vessels is not taken into account with these straight 3-D IVUS methods, this limitation can be overcome by fusing the curvature information provided by biplane angiography or other techniques with the IVUS border information (Schuurbiers et al., 2009; Sherknies et al., 2005; Tu et al., 2010; Wahle et al., 2006). To do so, one common method is to acquire two separate angiographic images from different angles at the beginning of the ultrasound scanning imaging procedure and to use the catheter outline reconstructed from these images as a template for placement of the IVUS-derived contours (Bourantas et al., 2005; Klingensmith et al., 2000b; Sherknies et al., 2005; von Birgelen et al., 1995; Weichert et al., 2003). Another method consists in following the IVUS transducer in time and space throughout the IVUS pullback using biplane angiography, thus the precise locations of IVUS image acquisitions are recorded in sequence and are used as a reconstruction template (Klingensmith et al., 2000b; Miyazaki et al., 2010; Wallace et al., 2005). However, this method might be difficult because of the cardiac and respiratory motion and the higher radiation exposure during the whole procedure.
Next to the precise location in 3-D space, other geometric considerations of the IVUS probe during image acquisition are important to be taken in account for an accurate 3-D reconstruction (Roelandt et al., 1994; Thrush et al., 1997). For example, the geometry of the reconstructed vessel can be distorted by a rotation of the catheter during pullback. These changes in the angular orientation of the catheter can be corrected by using analytical calculation based on the Frenet-Serret rules and optimizing the fit after projecting the reconstructed lumen from different rotational angles onto the angiogram images (Briguori et al., 2001; Wahle et al., 1999). Axial movements of the catheter due to the cardiac contraction are another cause for 3-D reconstruction inaccuracies. This geometric artifact can be reduced using a cardiac-gating and spatiotemporal location of the IVUS transducer throughout the pullback (Arbab-Zadeh et al., 1999). However, even if some errors in generating 3-D images can potentially surround withy these geometric assumptions, these corrections help improve the interpretability, usefulness and accuracy of the 3-D reconstructions. Repeatability is also a really important consideration in the accuracy and usefulness of 3-D reconstruction techniques. This aspect is however closely related to the reproducibility of the 3-D border-detection process (von Birgelen et al., 1996a).
Offline digitization of IVUS images and retrieval of biplane angiographic images, but also digitization and intense computer processing are both required to obtain a correct

geometrically 3-D reconstruction (Prati et al., 1998). Therefore, all these factors, in addition to the artifacts induced by the respiratory and cardiac motions, limit the *in vivo* applicability of the techniques. Other developments of real-time transducer tracking and online radiofrequency IVUS data acquisition can be integrated into the IVUS console to provide accurate 3-D models of investigated vessels within a few minutes after the acquisition (Nair et al., 2002). These add-ons seem really powerful since they could provide an interactive tool for assessing the diagnostic of the pathology, giving an assessment of luminal dimensions, but also vessel and plaque size from any viewing angle and position. Furthermore, these interactive models could allow rotation and manipulation of these virtual 3-D models on the console computer, authorizing the placement of a virtual stent inside the reconstructed artery, thus permitting a stent with the length and size to be appropriately chosen (Atary et al., 2009; Hong et al., 2010).
Other addendum could be integrated into the geometrically correct 3-D models, including analysis of hemodynamic forces, radiofrequency-derived histology, and 3-D stress maps. Therefore, a more precise morphologic plaque classification is possible with the analysis of radiofrequency data. In fact, the back-scattered radiofrequency IVUS data seems to permit the precise characterization of plaque composition, distinguishing the regions of calcified plaque *vs.* calcified necrosis *vs.* collagen (Nair et al., 2001). Another complement might consist on adding the mechanical properties of the investigated tissue. In fact, elastography represents the way a given tissue is responding to an applied force, as a function of its mechanical properties. Thus, the local mechanical properties of the tissue can be determined by comparing the images of a vessel acquired at 2 different levels of static compression (*e.g.* during systole and diastole steps of the cardiac cycle). This strain image (elastogram) may allow a better understanding of the relation between the progression of a disease and the *in vivo* mechanical properties of the vessel (Baldewsing et al., 2007; Cespedes et al., 1997; de Korte & van der Steen, 2002; Liang et al., 2008).

4.4 Comparison of IVUS with other imaging modalities

Even if IVUS might represent the most clinically established technique, other methodologies for vessel investigation are also available, such as angiography or tomographic imaging with magnetic resonance imaging (MRI) and computed tomography (CT). The current IVUS imaging plane resolution achieved in vessel cross sections is of 50 to 150 μm, whereas current frame rates (typically 30 frames/s), pullback speeds (usually 0.5 mm/s), and an ECG-gating or sub-sampling yield images at approximately 0.5- to 1.0-mm intervals (Gatta et al., 2009). On the other hand, the in-plane resolution of magnetic resonance imaging is around 1 mm and the through-plane resolution is between 3 to 5 mm with 2-D techniques (Escolar et al., 2006; Schaar et al., 2007), but the magnetic resonance imaging may allow, under several limitation in spatial resolution and signal-to-noise ratios, the atherosclerotic plaque components to be distinguished (Karmonik et al., 2006). At last, the in-plane resolution of computed tomography is less than 1 mm and the minimum through-plane resolution is approximately 1.25 to 1.50 mm. Some contrast-enhanced protocols are sometimes used to differentiate calcified and non-calcified plaque using contrast agents during computed tomography imaging of vessels (Nasir et al., 2010; Pundziute et al., 2008).
Another important difference between IVUS and the other imaging modalities concerns the orientation of the imaging plane. In fact, since the IVUS probe is inside the vessel during the acquisition, the IVUS imaging plane is oriented perpendicular to the vessel axis, which is optimal for assessing cross-sectional dimensions. On the other hand, magnetic resonance

images can be acquired along some body axes (e.g. axial, sagittal, or coronal planes or in a plane oblique to these orthogonal planes) and computed tomography images are typically only acquired in the axial plane, but these images can be reformatted to another orthogonal plane or an oblique plane with image processing techniques (McPherson et al., 2005). Therefore, these plane or oblique images allow only the measurement of relatively short portions of a vessel (only for images that are perpendicular to the vessel axis) and the curvature of the vessel introduces angulation errors in parameter measurement such as the wall thickness (Sherknies et al., 2005).

4.5 Color IVUS and virtual histology IVUS

Color flow IVUS is produced by computer software that detects a difference between the movements of echogenic blood particles from two sequential adjacent frames. Then the blood flow is colored by the software in a red or bleu and is displayed as axial and 3D longitudinal renderings with a very high image resolution (McLeod et al., 2004; Nair et al., 2002). The rendering color of the flow may change from red to orange when there is very fast blood flow (e.g., a tight stenosis). However, the flow velocities cannot be calculated with this technique, image resolution is very high. The color flow IVUS is available on Eagle Eye Gold and the Visions PV 018 catheters (Volcano Corporation, Rancho Cordova, CA) (see Table 1 for specifications). During a color flow IVUS pull-back, the blood flow is displayed in the vessel lumen, pulsing with each cardiac cycle. Unfortunately, the color flow is not gated with the heart rate and cannot be performed when virtual histology images are being acquired. These color flow IVUS are the helpful in distinguishing echolucent disease from luminal blood flow and can also be used to perform peripheral interventions in patients with renal failure or allergy, avoiding the use of contrast media (Goderie et al., 2010; Irshad et al., 2001).

Whereas conventional grayscale ultrasound images are generated from the intensity of the reflected signals that are collected by the probe, virtual histology IVUS images are obtained from the frequency and intensity of the returning signals and frequency varies depending on the tissues (Vince & Davies, 2004). An histological classification has then be realized by comparing the reflected virtual histology data with true histological sections of diseased vessels, and a color-coded map of the different components of the arterial disease has been established (dark green, fibrous; yellow/green, fibro-fatty; white, calcified; red, necrotic lipid core plaque) (McLeod et al., 2004; Nair et al., 2002). This color-coded map is of major importance since it allows the operator to have detailed information about the constituents and the nature of the plaque (Sarno et al., 2011). The virtual histology IVUS is available on Eagle Eye Gold catheter (Volcano Corporation, Rancho Cordova, CA) (see Table 1 for specifications) and is gated with the heartbeat. During the procedure using the "Volcano" setting, the segment length of the vessel to be examined is determined and the luminal border and the external elastic lamina border of the artery are automatically detected by the edge-tracking computer software but might require some manual adjustments. Then, virtual histology images of the delineated plaque can then be processed online with a few minutes, thus allowing clinical decisions to be made promptly, whereas some additional processing can be done offline (Vince & Davies, 2004).

5. Therapeutic interventions

5.1 Percutaneous trans-luminal angioplasty

The accurate measurement of the true luminal diameter, the assessment of the calcific nature of the plaque, the precise delineation of wall morphology, and the ability to carefully

visualize the post-balloon result are both required for a successful percutaneous trans-luminal angioplasty of peripheral arterial lesions. In that purpose, IVUS images can delineate the luminal and adventitial surfaces of vessel segments, can discriminate between normal and diseased components, can accurately localization and measurement of the thickness of plaque, and can also differentiate calcified and non-calcified vascular lesions (Pundziute et al., 2008; Rodriguez-Granillo et al., 2006). In fact, since the ultrasound energy is strongly reflected by calcified plaque, it appears as a very bright image with dense acoustic shadowing behind it. Not only luminal dimensions and wall thickness determined by IVUS are accurate to within 0.05 mm (Rodriguez-Granillo et al., 2006), the luminal cross-sectional areas measured from IVUS correlate well with calculated from biplanar angiograms (Cooper et al., 2001; Irshad et al., 2001). Therefore, IVUS allows the sized balloon or stent to be appropriately chosen can whereas conventional angiography is somewhat limited in its ability to provide sensitive data regarding the effects of percutaneous trans-luminal angioplasty. The IVUS advantage is also to provide a precise evaluation of the lesion morphology, such as the luminal dimensions, the trans-mural lesion characteristics and the area of blood flow. Furthermore, the IVUS determination of plaque volume before and after the procedure offers a real quantitative method to estimate the amount of lesion debulking or displacement and a reference point from which to assess the lesion recurrence/restenosis (Kim et al., 2004; Takeda et al., 2003).

The adjunctive use of IVUS during percutaneous trans-luminal angioplasty has been reported on several studies. For example, in patients with lesions of the superficial femoral artery treated with percutaneous trans-luminal angioplasty, IVUS has been reported to accurately detect the presence of dissections, plaque fractures, internal elastic lamina ruptures, and thinning of the media that occurred during the balloon angioplasty (Oshima et al., 1998; Tang et al., 2010). IVUS has also showed that, after a percutaneous trans-luminal angioplasty, the luminal enlargement is mainly produced by stretching of the arterial wall while the volume of the lesion remains relatively constant (Tang et al., 2010).

After a percutaneous trans-luminal angioplasty the restenosis risk has also been correlated to IVUS findings during the initial procedure, providing important information regarding the post-procedural follow-up and surveillance (Montorsi et al., 2004; Xu et al., 1995). The percutaneous trans-luminal angioplasty of a calcific plaque leads to a higher incidence of dissection than a fibrous lesion, whereas fibrous plaques or concentric lesions without signs of fracture or dissection are prone to have late restenosis after a percutaneous trans-luminal angioplasty (Garcia-Garcia et al., 2009; Su et al., 2009). In the same way, IVUS is also able to readily identify that early restenosis following interventions is associated with luminal thrombus, extensive dissection, and oversized balloon dilatation, while late restenosis correlates with residual stenosis, lower residual lumen surface, undersized balloon use, concentric fibrous plaque, absence of dissection, and absence of calcification (Irshad et al., 2001). IVUS is thus able to enhance percutaneous trans-luminal angioplasty procedures by allowing peri-procedural decisions to be made regarding the need for additional interventions.

5.2 Intravascular stents

Dissections, elastic recoil, residual stenosis, a significant residual pressure gradient across the lesion, or plaque ulceration with local thrombus accumulation are common indications for an intravascular stent placement after percutaneous trans-luminal angioplasty. Primary stenting is also commonly used in the treatment of certain lesions, especially common iliac or renal disease (Moise et al., 2009). These intravascular stents are used to increase the

patency of arterial occlusive lesions that have undergone angioplasty by reducing technical failure and restenosis rates. However, placing stents is not without risk since ineffective stent expansion can lead to early thrombosis or a stent migration, whereas overexpansion can result in vessel perforation or excessive intimal hyperplasia (Adlakha et al., 2010).
Establishing the need for stenting as well as the guiding of a stent deployment has been clearly helped by IVUS. Furthermore, defining the appropriate angioplasty diameter endpoint and confirming adequacy of stent deployment have been reported to clearly improve the long-term patency of a vessel undergoing balloon angioplasty and stenting (Waksman et al., 2009).

5.3 Venous interventions

The requirement of IVUS in endovascular interventions of venous disease is not as well described as for arterial lesions, while there are many useful indications for IVUS use in venous obstructive lesions (Raju et al., 2010; Raju & Neglen, 2006). In fact, traditional venography for iliac vein obstruction has numerous limitations, and IVUS imaging yields findings not obvious on venography . In fact, intra-luminal webs or external compression and subsequent deformity represent abnormalities that might disturb the diagnostic. Thus, IVUS can provide an accurate assessment of the degree of vein stenosis whereas the venography can sometimes underestimates this stenosis degree by 30% (Nair et al., 2002). In the same way, IVUS allows more appropriately sized venous stents to be placed after venoplasty. Since more and more venous interventions are being performed for acute deep venous thromboses, effort thromboses, or congenital stenosis, the requirement IVUS might represent a powerful adjunct to delineate the often unclear anatomy related to the venous system (Raju et al., 2010).

6. Conclusion

IVUS requirement has moved rapidly from a purely diagnostic imaging modality to a useful adjunct for vessel endografting to playing an ever-increasing role in peripheral occlusive interventions. This shift has been mainly supported by the miniaturization of the elements, allowing the device and catheter to be as small-profile as the latest stents or balloons, and by the powerful helped that can give IVUS for the most optimal outcomes. While vascular interventions are becoming more and more complex and venture into smaller target vessels, success will be related to the degree of accuracy of the guidance system employed during the procedure. Thus, IVUS is representing an important component of current and future endovascular interventions and should be integrated into the routine practice of the advanced endovascular surgeon and training programs.

7. References

Adlakha, S., Sheikh, M., Wu, J., Burket, M.W., Pandya, U., Colyer, W., Eltahawy, E., & Cooper, C.J. (2010). Stent fracture in the coronary and peripheral arteries. *J Interv Cardiol*, Vol. 23, No. 4, (Publication date: 2010/09/02), pp. 411-419, I.S.S.N.: 1540-8183

Allan, J.J., Smith, R.S., DeJong, S.C., McKay, C.R., & Kerber, R.E. (1998). Intracardiac echocardiographic imaging of the left ventricle from the right ventricle: quantitative experimental evaluation. *J Am Soc Echocardiogr*, Vol. 11, No. 10, (Publication date: 1998/11/06), pp. 921-928, I.S.S.N.: 0894-7317

Arbab-Zadeh, A., DeMaria, A.N., Penny, W.F., Russo, R.J., Kimura, B.J., & Bhargava, V. (1999). Axial movement of the intravascular ultrasound probe during the cardiac cycle: implications for three-dimensional reconstruction and measurements of coronary dimensions. *Am Heart J*, Vol. 138, No. 5 Pt 1, (Publication date: 1999/10/28), pp. 865-872, I.S.S.N.: 0002-8703

Atary, J.Z., Bergheanu, S.C., van der Hoeven, B.L., Atsma, D.E., Bootsma, M., van der Kley, F., Zeppenfeld, K., Jukema, J.W., & Schalij, M.J. (2009). Impact of sirolimus-eluting stent implantation compared to bare-metal stent implantation for acute myocardial infarction on coronary plaque composition at nine months follow-up: a Virtual Histology intravascular ultrasound analysis. Results from the Leiden MISSION! intervention study. *EuroIntervention*, Vol. 5, No. 5, (Publication date: 2010/02/10), pp. 565-572, I.S.S.N.: 1969-6213

Baldewsing, R.A., Schaar, J.A., Mastik, F., & van der Steen, A.F. (2007). Local elasticity imaging of vulnerable atherosclerotic coronary plaques. *Adv Cardiol*, Vol. 44, No. (Publication date: 2006/11/01), pp. 35-61, I.S.S.N.: 0065-2326

Bourantas, C.V., Kourtis, I.C., Plissiti, M.E., Fotiadis, D.I., Katsouras, C.S., Papafaklis, M.I., & Michalis, L.K. (2005). A method for 3D reconstruction of coronary arteries using biplane angiography and intravascular ultrasound images. *Comput Med Imaging Graph*, Vol. 29, No. 8, (Publication date: 2005/11/10), pp. 597-606, I.S.S.N.: 0895-6111

Bovenkamp, E.G., Dijkstra, J., Bosch, J.G., & Reiber, J.H. (2009). User-agent cooperation in multiagent IVUS image segmentation. *IEEE Trans Med Imaging*, Vol. 28, No. 1, (Publication date: 2009/01/01), pp. 94-105, I.S.S.N.: 1558-0062

Briguori, C., Anzuini, A., Airoldi, F., Gimelli, G., Nishida, T., Adamian, M., Corvaja, N., Di Mario, C., & Colombo, A. (2001). Intravascular ultrasound criteria for the assessment of the functional significance of intermediate coronary artery stenoses and comparison with fractional flow reserve. *Am J Cardiol*, Vol. 87, No. 2, (Publication date: 2001/01/12), pp. 136-141, I.S.S.N.: 0002-9149

Bruining, N., von Birgelen, C., de Feyter, P.J., Ligthart, J., Li, W., Serruys, P.W., & Roelandt, J.R. (1998). ECG-gated versus nongated three-dimensional intracoronary ultrasound analysis: implications for volumetric measurements. *Cathet Cardiovasc Diagn*, Vol. 43, No. 3, (Publication date: 1998/04/16), pp. 254-260, I.S.S.N.: 0098-6569

Cardinal, M.H., Soulez, G., Tardif, J.C., Meunier, J., & Cloutier, G. (2010). Fast-marching segmentation of three-dimensional intravascular ultrasound images: a pre- and post-intervention study. *Med Phys*, Vol. 37, No. 7, (Publication date: 2010/09/14), pp. 3633-3647, I.S.S.N.: 0094-2405

Cavaye, D.M., White, R.A., Kopchok, G.E., Mueller, M.P., Maselly, M.J., & Tabbara, M.R. (1992). Three-dimensional intravascular ultrasound imaging of normal and diseased canine and human arteries. *J Vasc Surg*, Vol. 16, No. 4, (Publication date: 1992/10/01), pp. 509-517; discussion 518-509, I.S.S.N.: 0741-5214

Cespedes, E.I., de Korte, C.L., van der Steen, A.F., von Birgelen, C., & Lancee, C.T. (1997). Intravascular elastography: principles and potentials. *Semin Interv Cardiol*, Vol. 2, No. 1, (Publication date: 1997/03/01), pp. 55-62, I.S.S.N.: 1084-2764

Chandrasekaran, K., Sehgal, C.M., Hsu, T.L., Young, N.A., D'Adamo, A.J., Robb, R.A., & Pandian, N.G. (1994). Three-dimensional volumetric ultrasound imaging of arterial pathology from two-dimensional intravascular ultrasound: an in vitro study.

Angiology, Vol. 45, No. 4, (Publication date: 1994/04/01), pp. 253-264, I.S.S.N.: 0003-3197

Cooper, B.Z., Kirwin, J.D., Panetta, T.F., Weinreb, F.M., Ramirez, J.A., Najjar, J.G., Blattman, S.B., Rodino, W., & Song, M. (2001). Accuracy of intravascular ultrasound for diameter measurement of phantom arteries. *J Surg Res*, Vol. 100, No. 1, (Publication date: 2001/08/23), pp. 99-105, I.S.S.N.: 0022-4804

Danilouchkine, M.G., Mastik, F., & van der Steen, A.F. (2009). Reconstructive compounding for IVUS palpography. *IEEE Trans Ultrason Ferroelectr Freq Control*, Vol. 56, No. 12, (Publication date: 2009/12/31), pp. 2630-2642, I.S.S.N.: 1525-8955

de Korte, C.L., & van der Steen, A.F. (2002). Intravascular ultrasound elastography: an overview. *Ultrasonics*, Vol. 40, No. 1-8, (Publication date: 2002/08/06), pp. 859-865, I.S.S.N.: 0041-624X

Di Mario, C., von Birgelen, C., Prati, F., Soni, B., Li, W., Bruining, N., de Jaegere, P.P., de Feyter, P.J., Serruys, P.W., & Roelandt, J.R. (1995). Three dimensional reconstruction of cross sectional intracoronary ultrasound: clinical or research tool? *Br Heart J*, Vol. 73, No. 5 Suppl 2, (Publication date: 1995/05/01), pp. 26-32, I.S.S.N.: 0007-0769

Diethrich, E.B. (1993). Endovascular treatment of abdominal aortic occlusive disease: the impact of stents and intravascular ultrasound imaging. *Eur J Vasc Surg*, Vol. 7, No. 3, (Publication date: 1993/05/01), pp. 228-236, I.S.S.N.: 0950-821X

Escolar, E., Weigold, G., Fuisz, A., & Weissman, N.J. (2006). New imaging techniques for diagnosing coronary artery disease. *CMAJ*, Vol. 174, No. 4, (Publication date: 2006/02/16), pp. 487-495, I.S.S.N.: 1488-2329

Finet, G., Weissman, N.J., Mintz, G.S., Satler, L.F., Kent, K.M., Laird, J.R., Adelmann, G.A., Ajani, A.E., Castagna, M.T., Rioufol, G., & Pichard, A.D. (2003). Mechanism of lumen enlargement with direct stenting versus predilatation stenting: influence of remodelling and plaque characteristics assessed by volumetric intracoronary ultrasound. *Heart*, Vol. 89, No. 1, (Publication date: 2002/12/17), pp. 84-90, I.S.S.N.: 1468-201X

Garcia-Garcia, H.M., Shen, Z., & Piazza, N. (2009). Study of restenosis in drug eluting stents: new insights from greyscale intravascular ultrasound and virtual histology. *EuroIntervention*, Vol. 5 Suppl D, No. (Publication date: 2009/09/17), pp. D84-92, I.S.S.N.: 1774-024X

Gatta, C., Pujol, O., Rodriguez Leor, O., Mauri Ferre, J., & Radeva, P. (2009). Fast rigid registration of vascular structures in IVUS sequences. *IEEE Trans Inf Technol Biomed*, Vol. 13, No. 6, (Publication date: 2009/08/01), pp. 1006-1011, I.S.S.N.: 1558-0032

Goderie, T.P., van Soest, G., Garcia-Garcia, H.M., Gonzalo, N., Koljenovic, S., van Leenders, G.J., Mastik, F., Regar, E., Oosterhuis, J.W., Serruys, P.W., & van der Steen, A.F. (2010). Combined optical coherence tomography and intravascular ultrasound radio frequency data analysis for plaque characterization. Classification accuracy of human coronary plaques in vitro. *Int J Cardiovasc Imaging*, Vol. 26, No. 8, (Publication date: 2010/04/17), pp. 843-850, I.S.S.N.: 1875-8312

Haas, C., Ermert, H., Holt, S., Grewe, P., Machraoui, A., & Barmeyer, J. (2000). Segmentation of 3D intravascular ultrasonic images based on a random field model. *Ultrasound Med Biol*, Vol. 26, No. 2, (Publication date: 2000/03/21), pp. 297-306, I.S.S.N.: 0301-5629

Hagenaars, T., Gussenhoven, E.J., van Essen, J.A., Seelen, J., Honkoop, J., & van der Lugt, A. (2000). Reproducibility of volumetric quantification in intravascular ultrasound

images. *Ultrasound Med Biol*, Vol. 26, No. 3, (Publication date: 2000/04/25), pp. 367-374, I.S.S.N.: 0301-5629

Hiro, T., Hall, P., Maiello, L., Itoh, A., Colombo, A., Jang, Y.T., Salmon, S.M., & Tobis, J.M. (1998). Clinical feasibility of 0.018-inch intravascular ultrasound imaging device. *Am Heart J*, Vol. 136, No. 6, (Publication date: 1998/12/08), pp. 1017-1020, I.S.S.N.: 0002-8703

Hong, Y.J., Jeong, M.H., Kim, S.W., Choi, Y.H., Ma, E.H., Ko, J.S., Lee, M.G., Park, K.H., Sim, D.S., Yoon, N.S., Yoon, H.J., Kim, K.H., Park, H.W., Kim, J.H., Ahn, Y., Cho, J.G., Park, J.C., & Kang, J.C. (2010). Relation between plaque components and plaque prolapse after drug-eluting stent implantation--virtual histology-intravascular ultrasound. *Circ J*, Vol. 74, No. 6, (Publication date: 2010/05/11), pp. 1142-1151, I.S.S.N.: 1347-4820

Irshad, K., Reid, D.B., Miller, P.H., Velu, R., Kopchok, G.E., & White, R.A. (2001). Early clinical experience with color three-dimensional intravascular ultrasound in peripheral interventions. *J Endovasc Ther*, Vol. 8, No. 4, (Publication date: 2001/09/13), pp. 329-338, I.S.S.N.: 1526-6028

Jensen, L.O., Maeng, M., Thayssen, P., Christiansen, E.H., Hansen, K.N., Galloe, A., Kelbaek, H., Lassen, J.F., & Thuesen, L. (2008). Neointimal hyperplasia after sirolimus-eluting and paclitaxel-eluting stent implantation in diabetic patients: the Randomized Diabetes and Drug-Eluting Stent (DiabeDES) Intravascular Ultrasound Trial. *Eur Heart J*, Vol. 29, No. 22, (Publication date: 2008/10/04), pp. 2733-2741, I.S.S.N.: 1522-9645

Jinzaki, M., Ido, K., Shinmoto, H., Nakatsuka, S., & Hiramatsu, K. (1993). [Advantages of intravascular ultrasound--preliminary experience in patients with peripheral and renal vascular disease]. *Nippon Igaku Hoshasen Gakkai Zasshi*, Vol. 53, No. 4, (Publication date: 1993/04/25), pp. 478-480, I.S.S.N.: 0048-0428

Karmonik, C., Basto, P., & Morrisett, J.D. (2006). Quantification of carotid atherosclerotic plaque components using feature space analysis and magnetic resonance imaging. *Conf Proc IEEE Eng Med Biol Soc*, Vol. 1, No. (Publication date: 2007/10/20), pp. 3102-3105, I.S.S.N.: 1557-170X

Kim, Y.H., Hong, M.K., Lee, S.W., Lee, C.W., Han, K.H., Kim, J.J., Park, S.W., Mintz, G.S., & Park, S.J. (2004). Randomized comparison of debulking followed by stenting versus stenting alone for ostial left anterior descending artery stenosis: intravascular ultrasound guidance. *Am Heart J*, Vol. 148, No. 4, (Publication date: 2004/10/02), pp. 663-669, I.S.S.N.: 1097-6744

Klingensmith, J.D., Shekhar, R., & Vince, D.G. (2000a). Evaluation of three-dimensional segmentation algorithms for the identification of luminal and medial-adventitial borders in intravascular ultrasound images. *IEEE Trans Med Imaging*, Vol. 19, No. 10, (Publication date: 2000/12/29), pp. 996-1011, I.S.S.N.: 0278-0062

Klingensmith, J.D., Vince, D.G., Kuban, B.D., Shekhar, R., Tuzcu, E.M., Nissen, S.E., & Cornhill, J.F. (2000b). Assessment of coronary compensatory enlargement by three-dimensional intravascular ultrasound. *Int J Card Imaging*, Vol. 16, No. 2, (Publication date: 2000/08/06), pp. 87-98, I.S.S.N.: 0167-9899

Koning, G., Dijkstra, J., von Birgelen, C., Tuinenburg, J.C., Brunette, J., Tardif, J.C., Oemrawsingh, P.W., Sieling, C., Melsa, S., & Reiber, J.H. (2002). Advanced contour detection for three-dimensional intracoronary ultrasound: a validation--in vitro and

in vivo. *Int J Cardiovasc Imaging*, Vol. 18, No. 4, (Publication date: 2002/07/19), pp. 235-248, I.S.S.N.: 1569-5794

Kovalski, G., Beyar, R., Shofti, R., & Azhari, H. (2000). Three-dimensional automatic quantitative analysis of intravascular ultrasound images. *Ultrasound Med Biol*, Vol. 26, No. 4, (Publication date: 2000/06/17), pp. 527-537, I.S.S.N.: 0301-5629

Laskey, W.K., Brady, S.T., Kussmaul, W.G., Waxler, A.R., Krol, J., Herrmann, H.C., Hirshfeld, J.W., Jr., & Sehgal, C. (1993). Intravascular ultrasonographic assessment of the results of coronary artery stenting. *Am Heart J*, Vol. 125, No. 6, (Publication date: 1993/06/01), pp. 1576-1583, I.S.S.N.: 0002-8703

Lekston, A., Chudek, J., Gasior, M., Wilczek, K., Wiecek, A., Kokot, F., Gierlotka, M., Niklewski, T., Fijalkowski, M., Szygula-Jurkiewicz, B., Wojnicz, R., Bialas, B., Osuch, M., Maciejewski, B., & Polonski, L. (2008). Angiographic and intravascular ultrasound assessment of immediate and 9-month efficacy of percutaneous transluminal renal artery balloon angioplasty with subsequent brachytherapy in patients with renovascular hypertension. *Kidney Blood Press Res*, Vol. 31, No. 5, (Publication date: 2008/09/06), pp. 291-298, I.S.S.N.: 1423-0143

Liang, Y., Zhu, H., & Friedman, M.H. (2008). Estimation of the transverse strain tensor in the arterial wall using IVUS image registration. *Ultrasound Med Biol*, Vol. 34, No. 11, (Publication date: 2008/07/16), pp. 1832-1845, I.S.S.N.: 1879-291X

Liu, J.B., Bonn, J., Needleman, L., Chiou, H.J., Gardiner, G.A., Jr., & Goldberg, B.B. (1999). Feasibility of three-dimensional intravascular ultrasonography: preliminary clinical studies. *J Ultrasound Med*, Vol. 18, No. 7, (Publication date: 1999/07/10), pp. 489-495, I.S.S.N.: 0278-4297

Luo, Z., Wang, Y., & Wang, W. (2003). Estimating coronary artery lumen area with optimization-based contour detection. *IEEE Trans Med Imaging*, Vol. 22, No. 4, (Publication date: 2003/05/31), pp. 564-566, I.S.S.N.: 0278-0062

Matar, F.A., Mintz, G.S., Douek, P., Farb, A., Virmani, R., Javier, S.P., Popma, J.J., Pichard, A.D., Kent, K.M., Satler, L.F., & et al. (1994). Coronary artery lumen volume measurement using three-dimensional intravascular ultrasound: validation of a new technique. *Cathet Cardiovasc Diagn*, Vol. 33, No. 3, (Publication date: 1994/11/01), pp. 214-220, I.S.S.N.: 0098-6569

McLeod, A.L., Watson, R.J., Anderson, T., Inglis, S., Newby, D.E., Northridge, D.B., Uren, N.G., & McDicken, W.N. (2004). Classification of arterial plaque by spectral analysis in remodelled human atherosclerotic coronary arteries. *Ultrasound Med Biol*, Vol. 30, No. 2, (Publication date: 2004/03/05), pp. 155-159, I.S.S.N.: 0301-5629

McPherson, A., Karrholm, J., Pinskerova, V., Sosna, A., & Martelli, S. (2005). Imaging knee position using MRI, RSA/CT and 3D digitisation. *J Biomech*, Vol. 38, No. 2, (Publication date: 2004/12/16), pp. 263-268, I.S.S.N.: 0021-9290

Mehran, R., Mintz, G.S., Hong, M.K., Tio, F.O., Bramwell, O., Brahimi, A., Kent, K.M., Pichard, A.D., Satler, L.F., Popma, J.J., & Leon, M.B. (1998). Validation of the in vivo intravascular ultrasound measurement of in-stent neointimal hyperplasia volumes. *J Am Coll Cardiol*, Vol. 32, No. 3, (Publication date: 1998/09/19), pp. 794-799, I.S.S.N.: 0735-1097

Min, P.K., Jung, J.H., Ko, Y.G., Choi, D., Jang, Y., & Shim, W.H. (2007). Effect of cilostazol on in-stent neointimal hyperplasia after coronary artery stenting: a quantative

coronary angiography and volumetric intravascular ultrasound study. *Circ J*, Vol. 71, No. 11, (Publication date: 2007/10/30), pp. 1685-1690, I.S.S.N.: 1346-9843

Miyazaki, S., Hiasa, Y., & Kishi, K. (2010). Very late thrombosis after subintimal sirolimus-eluting stent implantation during percutaneous coronary intervention for chronic total occlusion. *J Invasive Cardiol*, Vol. 22, No. 8, (Publication date: 2010/08/04), pp. E162-165, I.S.S.N.: 1557-2501

Moise, M.A., Alvarez-Tostado, J.A., Clair, D.G., Greenberg, R.K., Lyden, S.P., Srivastava, S.D., Eagleton, M., Sarac, T.S., & Kashyap, V.S. (2009). Endovascular management of chronic infrarenal aortic occlusion. *J Endovasc Ther*, Vol. 16, No. 1, (Publication date: 2009/03/14), pp. 84-92, I.S.S.N.: 1526-6028

Montorsi, P., Galli, S., Fabbiocchi, F., Trabattoni, D., Ravagnani, P.M., & Bartorelli, A.L. (2004). Randomized trial of conventional balloon angioplasty versus cutting balloon for in-stent restenosis. Acute and 24-hour angiographic and intravascular ultrasound changes and long-term follow-up. *Ital Heart J*, Vol. 5, No. 4, (Publication date: 2004/06/10), pp. 271-279, I.S.S.N.: 1129-471X

Murata, T., Hiro, T., Fujii, T., Yasumoto, K., Murashige, A., Kohno, M., Yamada, J., Miura, T., & Matsuzaki, M. (2002). Impact of the cross-sectional geometry of the post-deployment coronary stent on in-stent neointimal hyperplasia: an intravascular ultrasound study. *Circ J*, Vol. 66, No. 5, (Publication date: 2002/05/28), pp. 489-493, I.S.S.N.: 1346-9843

Nair, A., Kuban, B.D., Obuchowski, N., & Vince, D.G. (2001). Assessing spectral algorithms to predict atherosclerotic plaque composition with normalized and raw intravascular ultrasound data. *Ultrasound Med Biol*, Vol. 27, No. 10, (Publication date: 2001/12/04), pp. 1319-1331, I.S.S.N.: 0301-5629

Nair, A., Kuban, B.D., Tuzcu, E.M., Schoenhagen, P., Nissen, S.E., & Vince, D.G. (2002). Coronary plaque classification with intravascular ultrasound radiofrequency data analysis. *Circulation*, Vol. 106, No. 17, (Publication date: 2002/10/23), pp. 2200-2206, I.S.S.N.: 1524-4539

Nasir, K., Rivera, J.J., Yoon, Y.E., Chang, S.A., Choi, S.I., Chun, E.J., Choi, D.J., Budoff, M.J., Blumenthal, R.S., & Chang, H.J. (2010). Variation in atherosclerotic plaque composition according to increasing coronary artery calcium scores on computed tomography angiography. *Int J Cardiovasc Imaging*, Vol. 26, No. 8, (Publication date: 2010/04/30), pp. 923-932, I.S.S.N.: 1875-8312

Nishanian, G., Kopchok, G.E., Donayre, C.E., & White, R.A. (1999). The impact of intravascular ultrasound (IVUS) on endovascular interventions. *Semin Vasc Surg*, Vol. 12, No. 4, (Publication date: 2000/01/29), pp. 285-299, I.S.S.N.: 0895-7967

Oshima, A., Itchhaporia, D., & Fitzgerald, P. (1998). New developments in intravascular ultrasound. *Vasc Med*, Vol. 3, No. 4, (Publication date: 1999/04/02), pp. 281-290, I.S.S.N.: 1358-863X

Papadogiorgaki, M., Mezaris, V., Chatzizisis, Y.S., Giannoglou, G.D., & Kompatsiaris, I. (2007). Texture Analysis and Radial Basis Function Approximation for IVUS Image Segmentation. *Open Biomed Eng J*, Vol. 1, No. (Publication date: 2007/01/01), pp. 53-59, I.S.S.N.: 1874-1207

Prati, F., Crea, F., Labellarte, A., Sommariva, L., Marino, P., Caradonna, E., Manzoli, A., Pappalardo, A., & Boccanelli, A. (2002). Normal distribution of an intravascular ultrasound index of vessel remodeling. *Ital Heart J*, Vol. 3, No. 12, (Publication date: 2003/03/04), pp. 710-714, I.S.S.N.: 1129-471X

Prati, F., Mallus, M.T., & Lioy, E. (1998). Three-dimensional reconstruction techniques applied to intracoronary images. *G Ital Cardiol*, Vol. 28, No. 4, (Publication date: 1998/06/09), pp. 460-467, I.S.S.N.: 0046-5968

Pundziute, G., Schuijf, J.D., Jukema, J.W., Decramer, I., Sarno, G., Vanhoenacker, P.K., Boersma, E., Reiber, J.H., Schalij, M.J., Wijns, W., & Bax, J.J. (2008). Evaluation of plaque characteristics in acute coronary syndromes: non-invasive assessment with multi-slice computed tomography and invasive evaluation with intravascular ultrasound radiofrequency data analysis. *Eur Heart J*, Vol. 29, No. 19, (Publication date: 2008/08/07), pp. 2373-2381, I.S.S.N.: 1522-9645

Raju, S., Darcey, R., & Neglen, P. (2010). Unexpected major role for venous stenting in deep reflux disease. *J Vasc Surg*, Vol. 51, No. 2, (Publication date: 2009/12/17), pp. 401-408; discussion 408, I.S.S.N.: 1097-6809

Raju, S., & Neglen, P. (2006). High prevalence of nonthrombotic iliac vein lesions in chronic venous disease: a permissive role in pathogenicity. *J Vasc Surg*, Vol. 44, No. 1, (Publication date: 2006/07/11), pp. 136-143; discussion 144, I.S.S.N.: 0741-5214

Reid, D.B., Douglas, M., & Diethrich, E.B. (1995). The clinical value of three-dimensional intravascular ultrasound imaging. *J Endovasc Surg*, Vol. 2, No. 4, (Publication date: 1995/11/01), pp. 356-364, I.S.S.N.: 1074-6218

Rodriguez-Granillo, G.A., McFadden, E.P., Aoki, J., van Mieghem, C.A., Regar, E., Bruining, N., & Serruys, P.W. (2006). In vivo variability in quantitative coronary ultrasound and tissue characterization measurements with mechanical and phased-array catheters. *Int J Cardiovasc Imaging*, Vol. 22, No. 1, (Publication date: 2005/12/20), pp. 47-53, I.S.S.N.: 1569-5794

Roelandt, J.R., di Mario, C., Pandian, N.G., Wenguang, L., Keane, D., Slager, C.J., de Feyter, P.J., & Serruys, P.W. (1994). Three-dimensional reconstruction of intracoronary ultrasound images. Rationale, approaches, problems, and directions. *Circulation*, Vol. 90, No. 2, (Publication date: 1994/08/01), pp. 1044-1055, I.S.S.N.: 0009-7322

Rosenfield, K., Kaufman, J., Pieczek, A.M., Langevin, R.E., Jr., Palefski, P.E., Razvi, S.A., & Isner, J.M. (1992). Human coronary and peripheral arteries: on-line three-dimensional reconstruction from two-dimensional intravascular US scans. Work in progress. *Radiology*, Vol. 184, No. 3, (Publication date: 1992/09/11), pp. 823-832, I.S.S.N.: 0033-8419

Rosenfield, K., Losordo, D.W., Ramaswamy, K., Pastore, J.O., Langevin, R.E., Razvi, S., Kosowsky, B.D., & Isner, J.M. (1991). Three-dimensional reconstruction of human coronary and peripheral arteries from images recorded during two-dimensional intravascular ultrasound examination. *Circulation*, Vol. 84, No. 5, (Publication date: 1991/11/01), pp. 1938-1956, I.S.S.N.: 0009-7322

Saketkhoo, R.R., Razavi, M.K., Padidar, A., Kee, S.T., Sze, D.Y., & Dake, M.D. (2004). Percutaneous bypass: subintimal recanalization of peripheral occlusive disease with IVUS guided luminal re-entry. *Tech Vasc Interv Radiol*, Vol. 7, No. 1, (Publication date: 2004/04/09), pp. 23-27, I.S.S.N.: 1089-2516

Sano, K., Mintz, G.S., Carlier, S.G., Fujii, K., Takebayashi, H., Kimura, M., Costa, J.R., Jr., Tanaka, K., Costa, R.A., Lui, J., Weisz, G., Moussa, I., Dangas, G.D., Mehran, R., Lansky, A.J., Kreps, E.M., Collins, M., Stone, G.W., Moses, J.W., & Leon, M.B. (2006). Volumetric intravascular ultrasound assessment of neointimal hyperplasia and nonuniform stent strut distribution in sirolimus-eluting stent restenosis. *Am J Cardiol*, Vol. 98, No. 12, (Publication date: 2006/12/06), pp. 1559-1562, I.S.S.N.: 0002-9149

Sanz-Requena, R., Moratal, D., Garcia-Sanchez, D.R., Bodi, V., Rieta, J.J., & Sanchis, J.M. (2007). Automatic segmentation and 3D reconstruction of intravascular ultrasound images for a fast preliminar evaluation of vessel pathologies. *Comput Med Imaging Graph*, Vol. 31, No. 2, (Publication date: 2007/01/12), pp. 71-80, I.S.S.N.: 0895-6111

Sarno, G., Garg, S., Gomez-Lara, J., Garcia Garcia, H.M., Ligthart, J., Bruining, N., Onuma, Y., Witberg, K., van Geuns, R.J., de Boer, S., Wykrzykowska, J., Schultz, C., Duckers, H.J., Regar, E., de Jaegere, P., de Feyter, P., van Es, G.A., Boersma, E., van der Giessen, W., & Serruys, P.W. (2011). Intravascular ultrasound radiofrequency analysis after optimal coronary stenting with initial quantitative coronary angiography guidance: an ATHEROREMO sub-study. *EuroIntervention*, Vol. 6, No. 8, (Publication date: 2011/02/19), pp. 977-984, I.S.S.N.: 1969-6213

Schaar, J.A., Mastik, F., Regar, E., den Uil, C.A., Gijsen, F.J., Wentzel, J.J., Serruys, P.W., & van der Stehen, A.F. (2007). Current diagnostic modalities for vulnerable plaque detection. *Curr Pharm Des*, Vol. 13, No. 10, (Publication date: 2007/04/14), pp. 995-1001, I.S.S.N.: 1873-4286

Schuurbiers, J.C., Lopez, N.G., Ligthart, J., Gijsen, F.J., Dijkstra, J., Serruys, P.W., Van der Steen, A.F., & Wentzel, J.J. (2009). In vivo validation of CAAS QCA-3D coronary reconstruction using fusion of angiography and intravascular ultrasound (ANGUS). *Catheter Cardiovasc Interv*, Vol. 73, No. 5, (Publication date: 2009/03/25), pp. 620-626, I.S.S.N.: 1522-726X

Scoccianti, M., Verbin, C.S., Kopchok, G.E., Back, M.R., Donayre, C.E., Sinow, R.M., & White, R.A. (1994). Intravascular ultrasound guidance for peripheral vascular interventions. *J Endovasc Surg*, Vol. 1, No. (Publication date: 1994/09/01), pp. 71-80, I.S.S.N.: 1074-6218

Shekhar, R., Cothren, R.M., Vince, D.G., Chandra, S., Thomas, J.D., & Cornhill, J.F. (1999). Three-dimensional segmentation of luminal and adventitial borders in serial intravascular ultrasound images. *Comput Med Imaging Graph*, Vol. 23, No. 6, (Publication date: 2000/01/14), pp. 299-309, I.S.S.N.: 0895-6111

Sherknies, D., Meunier, J., Mongrain, R., & Tardif, J.C. (2005). Three-dimensional trajectory assessment of an IVUS transducer from single-plane cineangiograms: a phantom study. *IEEE Trans Biomed Eng*, Vol. 52, No. 3, (Publication date: 2005/03/12), pp. 543-549, I.S.S.N.: 0018-9294

Siegel, R.J., Swan, K., Edwalds, G., & Fishbein, M.C. (1985). Limitations of postmortem assessment of human coronary artery size and luminal narrowing: differential effects of tissue fixation and processing on vessels with different degrees of atherosclerosis. *J Am Coll Cardiol*, Vol. 5, No. 2 Pt 1, (Publication date: 1985/02/01), pp. 342-346, I.S.S.N.: 0735-1097

Sonka, M., Liang, W., Kanani, P., Allan, J., DeJong, S., Kerber, R., & McKay, C. (1998). Intracardiac echocardiography: computerized detection of left ventricular borders. *Int J Card Imaging*, Vol. 14, No. 6, (Publication date: 1999/08/24), pp. 397-411, I.S.S.N.: 0167-9899

Su, J.L., Wang, B., & Emelianov, S.Y. (2009). Photoacoustic imaging of coronary artery stents. *Opt Express*, Vol. 17, No. 22, (Publication date: 2009/12/10), pp. 19894-19901, I.S.S.N.: 1094-4087

Takagi, A., Hibi, K., Zhang, X., Teo, T.J., Bonneau, H.N., Yock, P.G., & Fitzgerald, P.J. (2000). Automated contour detection for high-frequency intravascular ultrasound imaging:

a technique with blood noise reduction for edge enhancement. *Ultrasound Med Biol*, Vol. 26, No. 6, (Publication date: 2000/09/21), pp. 1033-1041, I.S.S.N.: 0301-5629

Takeda, Y., Tsuchikane, E., Kobayashi, T., Terai, K., Kobayashi, Y., Nakagawa, T., Sakurai, M., & Awata, N. (2003). Effect of plaque debulking before stent implantation on in-stent neointimal proliferation: a serial 3-dimensional intravascular ultrasound study. *Am Heart J*, Vol. 146, No. 1, (Publication date: 2003/07/10), pp. 175-182, I.S.S.N.: 1097-6744

Tang, G.L., Chin, J., & Kibbe, M.R. (2010). Advances in diagnostic imaging for peripheral arterial disease. *Expert Rev Cardiovasc Ther*, Vol. 8, No. 10, (Publication date: 2010/10/13), pp. 1447-1455, I.S.S.N.: 1744-8344

Thrush, A.J., Bonnett, D.E., Elliott, M.R., Kutob, S.S., & Evans, D.H. (1997). An evaluation of the potential and limitations of three-dimensional reconstructions from intravascular ultrasound images. *Ultrasound Med Biol*, Vol. 23, No. 3, (Publication date: 1997/01/01), pp. 437-445, I.S.S.N.: 0301-5629

Tu, S., Huang, Z., Koning, G., Cui, K., & Reiber, J.H. (2010). A novel three-dimensional quantitative coronary angiography system: In-vivo comparison with intravascular ultrasound for assessing arterial segment length. *Catheter Cardiovasc Interv*, Vol. 76, No. 2, (Publication date: 2010/07/29), pp. 291-298, I.S.S.N.: 1522-726X

Vince, D.G., & Davies, S.C. (2004). Peripheral application of intravascular ultrasound virtual histology. *Semin Vasc Surg*, Vol. 17, No. 2, (Publication date: 2004/06/09), pp. 119-125, I.S.S.N.: 0895-7967

von Birgelen, C., de Feyter, P.J., de Vrey, E.A., Li, W., Bruining, N., Nicosia, A., Roelandt, J.R., & Serruys, P.W. (1997a). Simpson's rule for the volumetric ultrasound assessment of atherosclerotic coronary arteries: a study with ECG-gated three-dimensional intravascular ultrasound. *Coron Artery Dis*, Vol. 8, No. 6, (Publication date: 1997/06/01), pp. 363-369, I.S.S.N.: 0954-6928

von Birgelen, C., Di Mario, C., Li, W., Schuurbiers, J.C., Slager, C.J., de Feyter, P.J., Roelandt, J.R., & Serruys, P.W. (1996a). Morphometric analysis in three-dimensional intracoronary ultrasound: an in vitro and in vivo study performed with a novel system for the contour detection of lumen and plaque. *Am Heart J*, Vol. 132, No. 3, (Publication date: 1996/09/01), pp. 516-527, I.S.S.N.: 0002-8703

von Birgelen, C., Di Mario, C., Reimers, B., Prati, F., Bruining, N., Gil, R., Serruys, P.W., & Roelandt, J.R. (1996b). Three-dimensional intracoronary ultrasound imaging. Methodology and clinical relevance for the assessment of coronary arteries and bypass grafts. *J Cardiovasc Surg (Torino)*, Vol. 37, No. 2, (Publication date: 1996/04/01), pp. 129-139, I.S.S.N.: 0021-9509

von Birgelen, C., Erbel, R., Di Mario, C., Li, W., Prati, F., Ge, J., Bruining, N., Gorge, G., Slager, C.J., Serruys, P.W., & et al. (1995). Three-dimensional reconstruction of coronary arteries with intravascular ultrasound. *Herz*, Vol. 20, No. 4, (Publication date: 1995/08/01), pp. 277-289, I.S.S.N.: 0340-9937

von Birgelen, C., Li, W., Bom, N., & Serruys, P.W. (1997b). Quantitative three-dimensional intravascular ultrasound. *Semin Interv Cardiol*, Vol. 2, No. 1, (Publication date: 1997/03/01), pp. 25-32, I.S.S.N.: 1084-2764

Wahle, A., Lopez, J.J., Olszewski, M.E., Vigmostad, S.C., Chandran, K.B., Rossen, J.D., & Sonka, M. (2006). Plaque development, vessel curvature, and wall shear stress in coronary arteries assessed by X-ray angiography and intravascular ultrasound. *Med*

Image Anal, Vol. 10, No. 4, (Publication date: 2006/04/29), pp. 615-631, I.S.S.N.: 1361-8415

Wahle, A., Prause, P.M., DeJong, S.C., & Sonka, M. (1999). Geometrically correct 3-D reconstruction of intravascular ultrasound images by fusion with biplane angiography--methods and validation. *IEEE Trans Med Imaging*, Vol. 18, No. 8, (Publication date: 1999/10/26), pp. 686-699, I.S.S.N.: 0278-0062

Waksman, R., Erbel, R., Di Mario, C., Bartunek, J., de Bruyne, B., Eberli, F.R., Erne, P., Haude, M., Horrigan, M., Ilsley, C., Bose, D., Bonnier, H., Koolen, J., Luscher, T.F., & Weissman, N.J. (2009). Early- and long-term intravascular ultrasound and angiographic findings after bioabsorbable magnesium stent implantation in human coronary arteries. *JACC Cardiovasc Interv*, Vol. 2, No. 4, (Publication date: 2009/05/26), pp. 312-320, I.S.S.N.: 1876-7605

Wallace, M.J., Ahrar, K., Tinkey, P., & Wright, K.C. (2005). Transvenous extrahepatic portacaval shunt with use of a modified prototype stent-graft: experimental study in animals. *J Vasc Interv Radiol*, Vol. 16, No. 2 Pt 1, (Publication date: 2005/02/17), pp. 261-267, I.S.S.N.: 1051-0443

Weichert, F., Muller, H., Quast, U., Kraushaar, A., Spilles, P., Heintz, M., Wilke, C., von Birgelen, C., Erbel, R., & Wegener, D. (2003). Virtual 3D IVUS vessel model for intravascular brachytherapy planning. I. 3D segmentation, reconstruction, and visualization of coronary artery architecture and orientation. *Med Phys*, Vol. 30, No. 9, (Publication date: 2003/10/08), pp. 2530-2536, I.S.S.N.: 0094-2405

White, R.A., Scoccianti, M., Back, M., Kopchok, G., & Donayre, C. (1994). Innovations in vascular imaging: arteriography, three-dimensional CT scans, and two- and three-dimensional intravascular ultrasound evaluation of an abdominal aortic aneurysm. *Ann Vasc Surg*, Vol. 8, No. 3, (Publication date: 1994/05/01), pp. 285-289, I.S.S.N.: 0890-5096

Xu, S., Nomura, M., Kurokawa, H., Ando, T., Kimura, M., Ishii, J., Hasegawa, H., Kondo, T., Tadiki, S., & Qi, P. (1995). Relationship between coronary angioscopic and intravascular ultrasound imaging and restenosis. *Chin Med J (Engl)*, Vol. 108, No. 10, (Publication date: 1995/10/01), pp. 743-749, I.S.S.N.: 0366-6999

Zhang, X., McKay, C.R., & Sonka, M. (1998). Tissue characterization in intravascular ultrasound images. *IEEE Trans Med Imaging*, Vol. 17, No. 6, (Publication date: 1999/02/27), pp. 889-899, I.S.S.N.: 0278-0062

Zimarino, M., Weissman, N.J., Waksman, R., De Caterina, R., Ahmed, J.M., Pichard, A.D., & Mintz, G.S. (2002). Analysis of stent edge restenosis with different forms of brachytherapy. *Am J Cardiol*, Vol. 89, No. 3, (Publication date: 2002/01/26), pp. 322-325, I.S.S.N.: 0002-9149

Zimmermann, A., Pollinger, B., Rieber, J., Konig, A., Erhard, I., Krotz, F., Sohn, H.Y., Kantlehner, R., Haimerl, W., Duhmke, E., Leibig, M., Theisen, K., Klauss, V., & Schiele, T.M. (2005). Early time course of neointima formation and vascular remodelling following percutaneous coronary intervention and vascular brachytherapy of in-stent restenotic lesions as assessed by intravascular ultrasound analysis. *Z Kardiol*, Vol. 94, No. 4, (Publication date: 2005/04/02), pp. 239-246, I.S.S.N.: 0300-5860

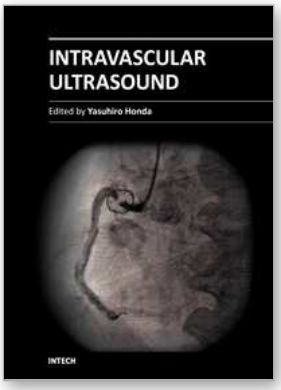

Intravascular Ultrasound

Edited by Dr. Yasuhiro Honda

ISBN 978-953-307-900-4
Hard cover, 207 pages
Publisher InTech
Published online 01, February, 2012
Published in print edition February, 2012

Intravascular ultrasound (IVUS) is a cardiovascular imaging technology using a specially designed catheter with a miniaturized ultrasound probe for the assessment of vascular anatomy with detailed visualization of arterial layers. Over the past two decades, this technology has developed into an indispensable tool for research and clinical practice in cardiovascular medicine, offering the opportunity to gather diagnostic information about the process of atherosclerosis in vivo, and to directly observe the effects of various interventions on the plaque and arterial wall. This book aims to give a comprehensive overview of this rapidly evolving technique from basic principles and instrumentation to research and clinical applications with future perspectives.

INTECH
open science | open minds

InTech Europe
University Campus STeP Ri
Slavka Krautzeka 83/A
51000 Rijeka, Croatia
Phone: +385 (51) 770 447
Fax: +385 (51) 686 166
www.intechopen.com

InTech China
Unit 405, Office Block, Hotel Equatorial Shanghai
No.65, Yan An Road (West), Shanghai, 200040, China
中国上海市延安西路65号上海国际贵都大饭店办公楼405单元
Phone: +86-21-62489820
Fax: +86-21-62489821